An Investigation into Optimal Subsonic Wing Sweep Angles

What is the effect of wing sweep angle at different subsonic speeds on the lift to drag ratio of a plane?

Table of Contents

Section 1: Introduction

Earlier this year, while watching an online MIT lecture by Randy Gordon about Lockheed Martin F-22 Raptor Flight Controls, I was inspired by the complexity of engineering involved in the production of these aircraft. I was specifically intrigued by the abnormal wing design that one sees only on these high speed fighter jets, reminding me of the Grumman F-14 Tomcat I had seen in the Air and Space Museum in California earlier, which has variable sweep angle wings. They can be adjusted from 20° which is closer to commercial aircraft to 68°. Since then I have wanted to take time to investigate this type of aircraft.

I became intrigued by the possibility of studying this in subsonic speeds because this is the region all commercial aircraft, which almost all have some degree of quarter chord sweep, spend the majority of their time flying in. The investigation of swept wings is also particularly important because it can minimize the total drag experienced by an aircraft, which if minimized without a significant decrease in lift could reduce overall fuel consumption and improve decrease environmental damage that aircraft cause. Fuel use is also crucial to the economy of commercial flying as reduced fuel consumption reduces cost. This led me to the research question: **What is the effect of wing sweep angle at different subsonic speeds on the lift to drag ratio of a plane?**

Section 2: Theoretical Background

Theories of Lift vary but are all contingent on either Bernoulli or Newton's laws, or a combination of both.

One model of lift is NASAs lift equation where C_L is the coefficient of lift, ρ is density of air, v is relative velocity and A is the surface area of the wings.

Equation 1: Lift Equation (Benson "The Lift Equation")

$$L = C_L \times \rho \times \frac{v^2}{2} \times A$$

This illustrates the factors that generate lift but does not describe the physics around the wing and how this is to be understood and applied. The following are the different theories that have been proposed, with some proving more useful than others.

One theory, the "equal transit time" or "longer path" (Benson "Bernoulli and Newton"), states that lift occurs due to air moving over the top of an airfoil faster than across the bottom of the airfoil. However, Bernoulli states that this occurs because the air molecules will start and end at the same time despite being on the top or the bottom and because the airfoil will have a longer path to travel over top of the wing, the air must be traveling faster.

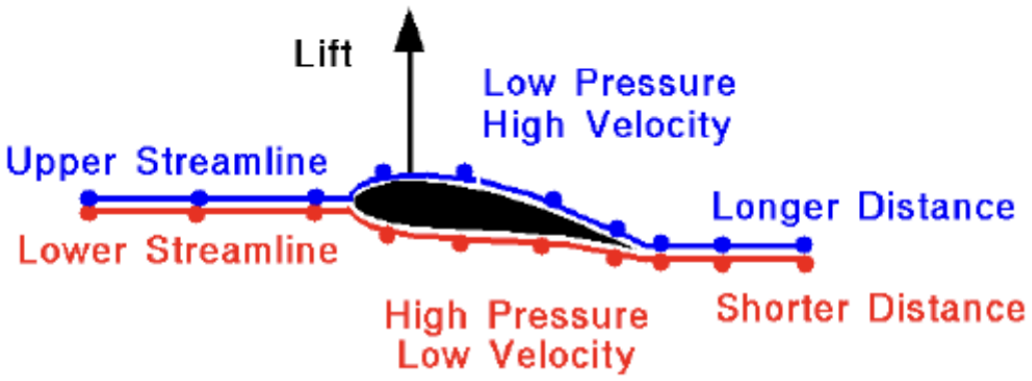

Figure 1: (Benson "Incorrect Theory #1")

Next, Bernoulli's model, which relates the velocity of a gas to its pressure, suggests that due to the low pressure area above, created by the increased velocity of the air, and the high pressure below, lift will be generated. This lift comes from the upwards force generated by a difference in pressure above and beneath the wing.

Equation 2: Bernoulli's Equation (Smits)

$$p + \frac{1}{2}\rho V^2 + \rho g h = constant$$

$$\frac{1}{2}\rho V^2 + \rho g h = constant$$

$$p_1 - p_2 = \frac{1}{2}p(V_2^2 - V_1^2)$$

$$A_1 V_1 = A_2 V_2$$

Where p is the pressure, ρ is the density, V is the velocity, and h is the elevation. From Equation 2, one can state the following relationships:

$$A_2 < A_1, P_2 < P_1, V_2 > V_1$$

This indicates that decreasing area will increase velocity and increasing velocity will lead to a decrease in pressure. This Equal Transit Time Theory has been proven false, however, in an experiment where smoke was injected into the airstream flowing over an airfoil (Babinsky). In image (*c*) one can see that the smoke does travel faster over the top as it has moved further in the same amount of time, but it has not reached the trailing edge at the same time.

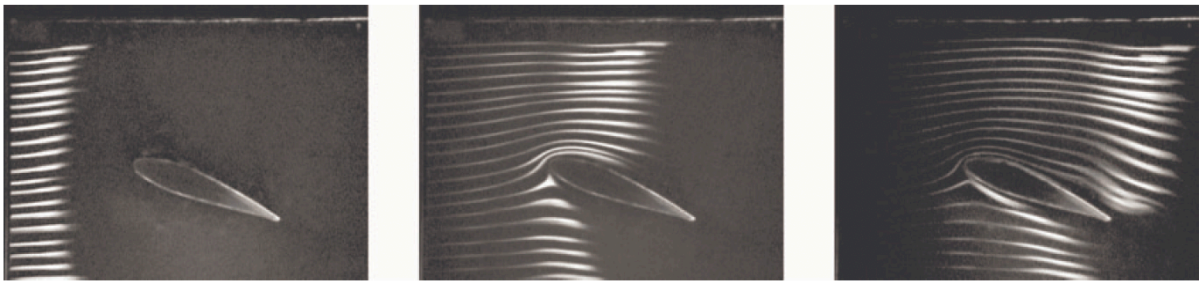

Figure 2: Smoke Flow Over an Airfoil (Babinsky 49)

A second theory, the "Venturi" theory, is based on the premise that the mass of air moving past a point will be constant in a Venturi Nozzle. This leads to the relationship that the mass flow rate (density times velocity times area) is a constant.

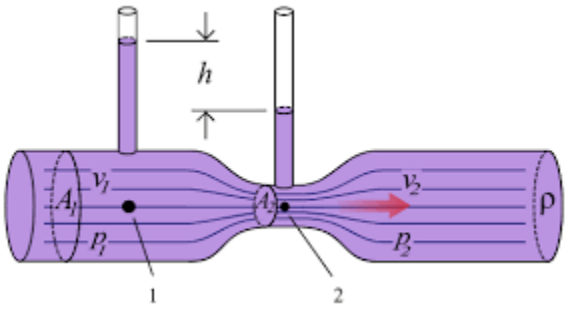

Figure 3: Diagram of Venturi Effect (HappyApple)

This applies well to a nozzle where the path of the airflow is constricted to a smaller area, thereby accelerating the airflow; this does not apply, however, to an airfoil as it will not behave like a nozzle. This is because there is enough space above the airfoil that the pressure and airfoil can disperse into open space.

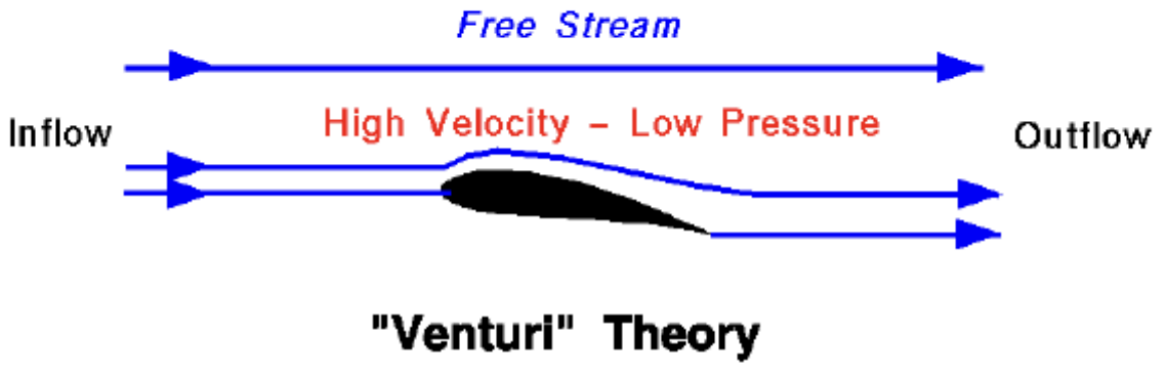

Figure 4: Diagram of Lift due to Newton's Third Law (Benson "Incorrect Theory #2")

Newton's third law which "equates aerodynamic lift to a stone skipping across the water" (Benson "Incorrect Theory #2") can be considered a third explanation; when wind hits the bottom of a wing, it gets deflected downward and by opposite force, the wing gets lift. This is not false, but it does not provide a comprehensive picture of the entire lift generation process because it neglects airflow above the wing (Benson "Bernoulli and Newton").

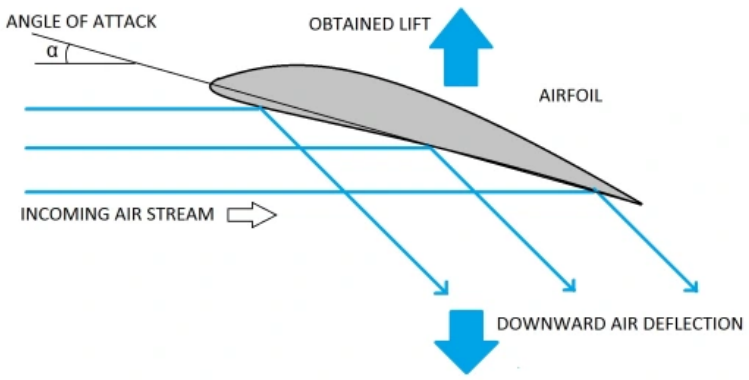

Figure 5: Diagram of Lift Generation due to Newton's Third Law (Cssonawala)

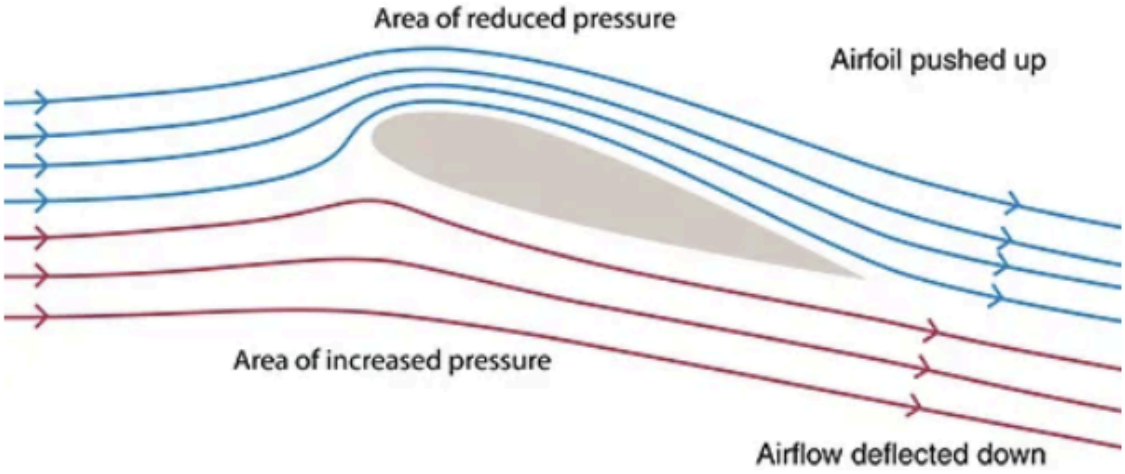

Figure 6: Diagram of Different Airspeeds and Pressures over an Airfoil (Burnside)

The most comprehensive explanation I found incorporates the theory that air flowing over a wing is turned by the curvature of the wing as it flows over and around the airfoil, eventually flowing off and downwards creating a "downwash" which, by Newton's Third Law, will induce an equal and opposite upward force, lift (Hall "What is Lift"). This upwards lift force is due to the difference in pressure above and below the wing. This difference in pressure arises from the increased velocity of airflow over the top of the wing, which Bernouilli's Equation states will result in decreased pressure.

One way of modeling drag is the NASA drag equation, similar to the lift equation (Equation 1), describes which factors influence the formation where C_d is the coefficient of drag and all other variables are the same as in Equation 1.

Equation 3: Drag Equation (Hall "Modern Drag Equation")

$$D = C_d \times \rho \times \frac{v^2}{2} \times A$$

$$D \propto C_d$$

Drag is primarily split into two types at low speeds: skin friction and form drag. Skin friction is the drag due to the air molecules traveling in contact with the airfoils surface resulting in friction and turbulent flow being generated in a layer due to the viscosity of the air. It is directly proportional to the area of the surface in contact with the air and increases with the square of the velocity ("Friction Drag"). Secondly, form drag is due to the air being obstructed and deflected by the shape of the airfoil altering the local velocity and pressure. Because pressure measures the momentum of the gas molecules and a change in momentum produces a force, varying pressure will produce a force on the airfoil known as form drag (Hall “What is Drag”)

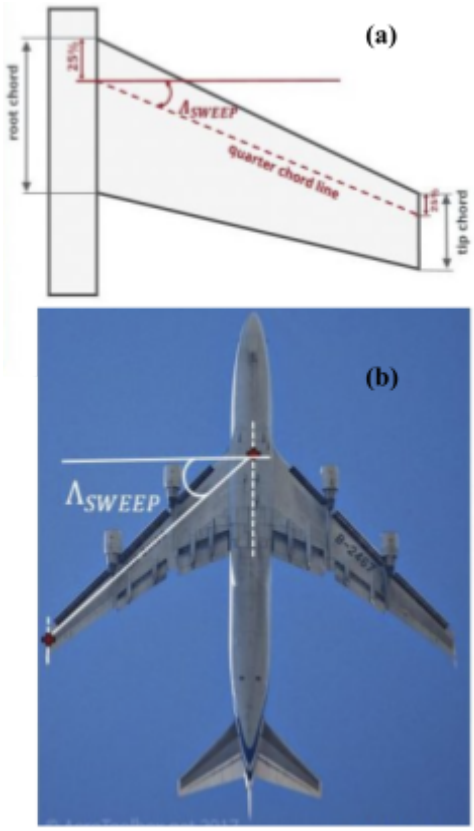

Figure 7: Diagrams Depicting Sweep Angle (Wood)

Sweep angle is most commonly defined as the angle between a perpendicular line with the root chord and the quarter chord line, which is a line between the quarter chord length of the wing root and the wing tip see Figures 7 (a) and (b). Sweep angle considerations become more critical as speed increases particularly when approaching mach speeds (343 ms^{-1}) but there are still significant measurable effects at subsonic speeds.

In terms of lift, an increase in sweep angle should always decrease the lift generated. This occurs because of the separation of just chordwise flow (airflow which is perpendicular to the leading edge of a wing) into multiple components of airflow: chordwise and spanwise ("Ask an Explainer"). Velocity vectors seen in Figure 8 illustrate how, because the airflow is split into two components, the chordwise flow velocity is decreased, as well as the mass of air going over the wing as some is redirected spanwise. Because the velocity and the mass of air moving over the wing decrease, the amount of downwash in terms of mass and velocity will be lower resulting in smaller lift force.

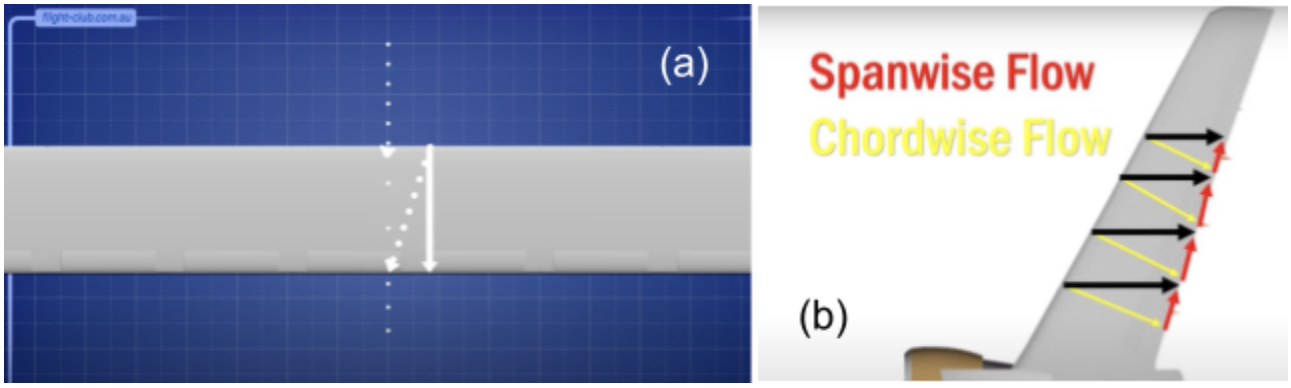

Figure 8: Diagrams of Spanwise and Chordwise Flow ("Swept Wings")

Skin drag will not significantly be affected as long as the planform area is kept the same; however, a form drag reduction should occur because the direction of the momentum of the deflected air by the face of the airfoil will not be directly opposing the wings direction of movement. As the sweep

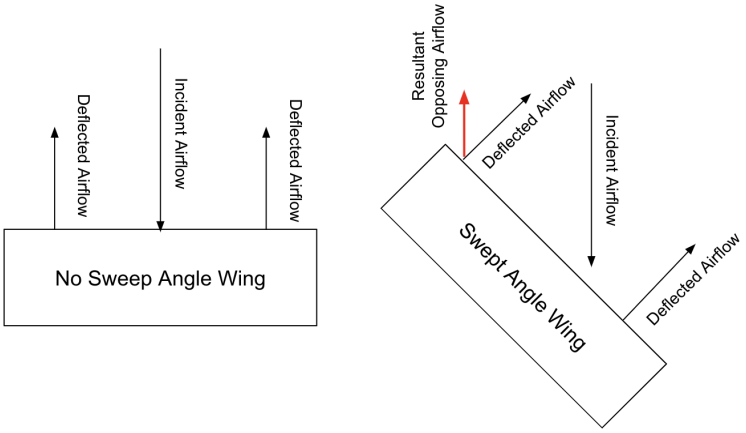

Figure 9: Diagram of Resultant Airflow Momentum (drawn on google drawings)

angle increases, the deflection of airflow will be directed outward away from the root of the wing and the resultant component direction of its momentum will be smaller (see Figure 8 (b)).

Section 3: Experiments and Investigation

3.1 Hypothesis

My initial hypothesis is that the lift data will follow a cos^2 relationship with sweep angle. This is based on a derivation of the coefficient of lift equation (Jing and Huang 969) shown in Equation 4, combined with $L \propto C_L$ Equation 1 (Benson "The Lift Equation"). Regarding sweep angles, previous researchers found the coefficient of lift can be given by (Jing and Huang 969), k being lift slope of the lift curve, α is angle of attack (AoA) and Λ is sweep angle, and C_{L0} is the lift coefficient when sweep angle $\Lambda = 0°$.

Equation 4: Coefficient of Lift against Sweep Angle (Jing and Huang 969)

$$C_L = (k\alpha + C_{L0})cos^2\Lambda$$

$$C_L \propto cos^2\Lambda$$

Additionally, many studies have demonstrated that lift generated by an airfoil will always decrease as sweep angle increases. In Figure 10, one can see that for different speeds, subsonic to transonic, the lift decreases as sweep angle increases.

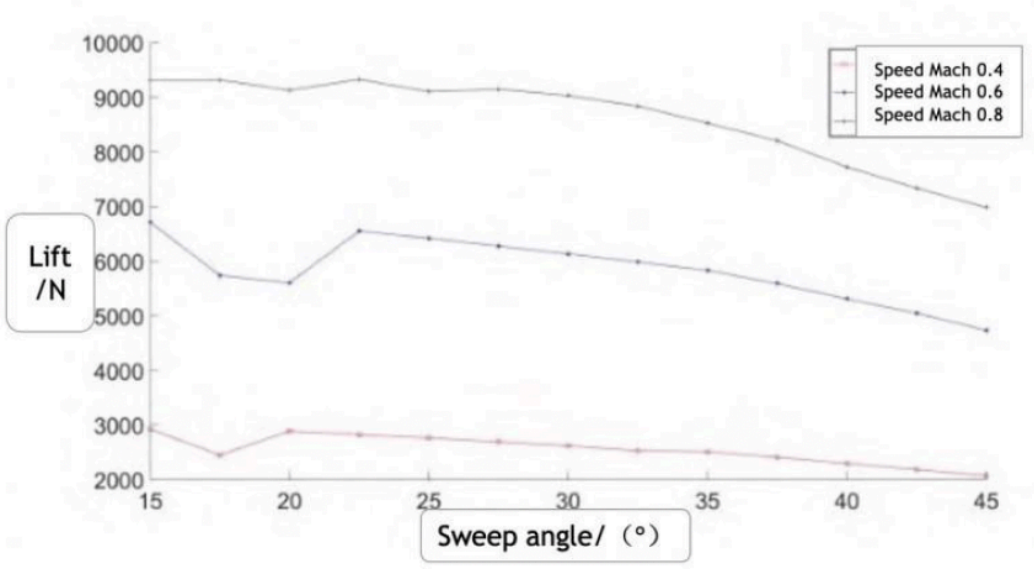

Figure 10: The Relationship Between Lift and Different Sweep Angles (Chen 75)

Further support is shown in Figure 11.

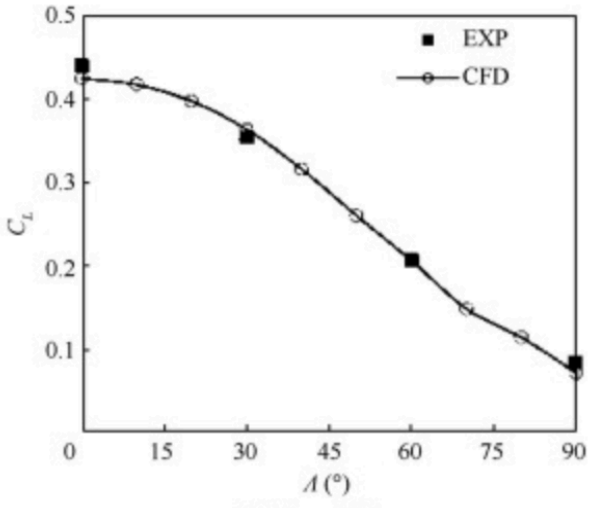

Figure 11: Comparison of Simulated Results with Experimental Data for Coefficient of Lift Under Different Sweep Angles (Zeng et al. 215)

There is no clear relationship between drag and sweep angle but data from Figures 12 and 13 can be referenced to support my hypothesis. Both graphs have the dependent variable drag coefficient (C_d), proportional to drag (Equation 3), therefore a decrease in drag coefficient shows a decrease in drag (assuming all other variables are kept constant). Figure 12 shows a small increase in the Drag coefficient for angles 0°- 60° and Figure 13 shows that for all measured speeds, the drag coefficient decreases as sweep angle increases.

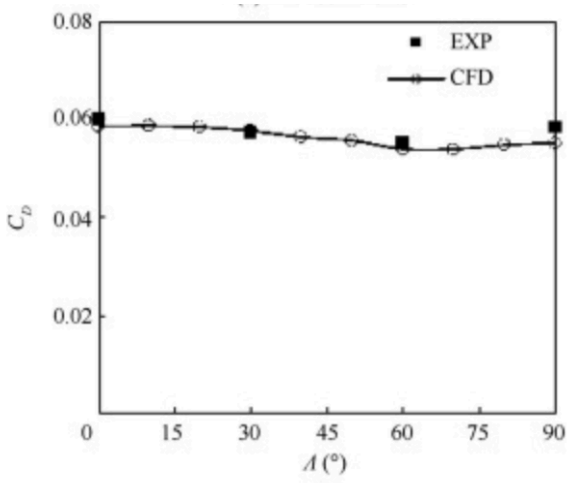

Figure 12: Drag Coefficient with Sweep Angle (Chen 76)

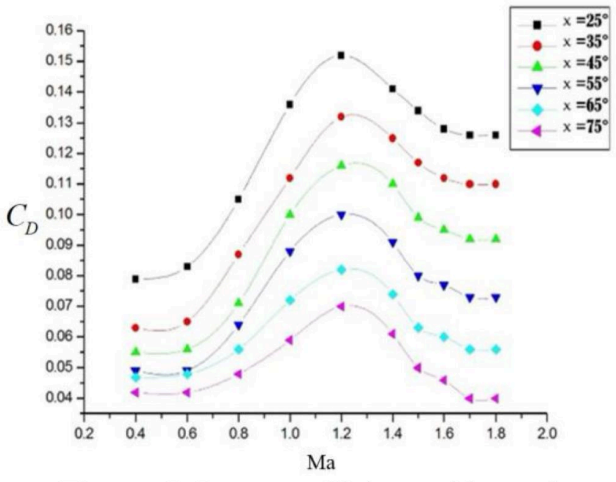

Figure 13: Drag Coefficient with Mach Number, AOA=12 (Lei et al. 4)

For lift-to-drag (L/D) ratio I predict that increasing the sweep angle of a wing in subsonic conditions will initially improve the L/D due to a reduction in form drag, but beyond a certain sweep angle, L/D will decrease as the reduction in lift outweighs the benefits of reduced drag. This suggests that there is an optimal sweep angle at which the aerodynamic efficiency is maximized, particularly in balancing lift and drag at various subsonic speeds. The evidence that a maximum L/D will be found is supported by Figures 14-17. In Figure 14 L/D max at 0.4 mach is

22.5°, L/D at 0.6 mach is 32.5° or 22.5°, L/D at 0.8 mach is 37.5° showing that for an increase in speed at subsonic speeds, the optimal sweep angle will increase.

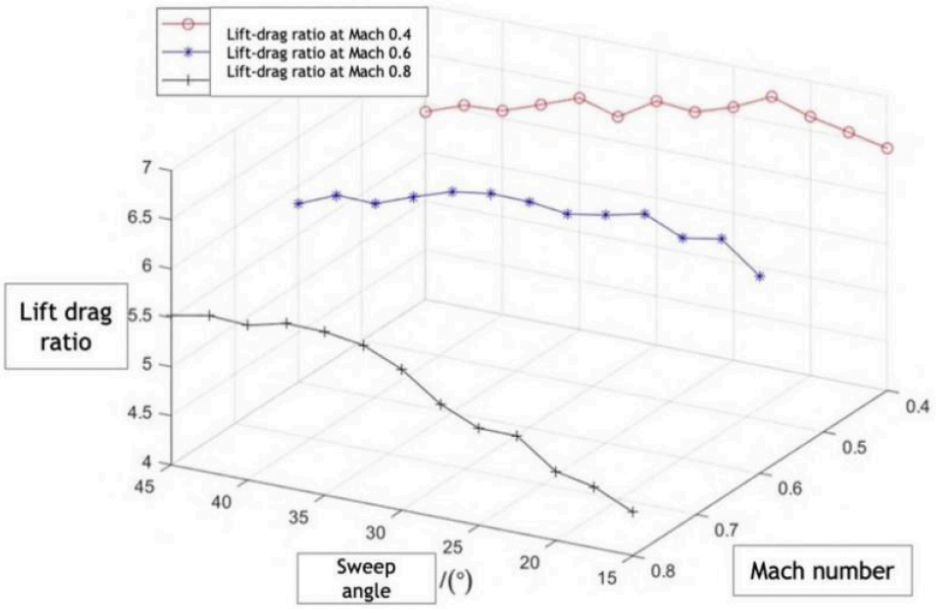

Figure 14: Lift-Drag Ratio of Variable-Sweep Wing Aircraft (Chen 78)

Additionally, Figures 15, 16 and 17 show that the optimal sweep angle for almost all angles of attack will increase as speed increases (Max L/D is at 25° at $M_a = 0.6$, at 35°-45° at 1 $M_a = 1$ and at 65° at $M_a = 1.4$); however, this data is less applicable as this data exceeds mach speeds where wave drag and shockwaves become a more significant factor.

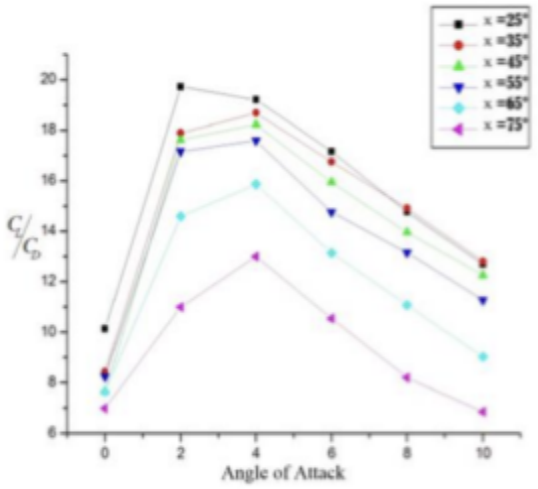

Fig 15: Lift-Drag Ratio with the AOA Ma=0.6

(Lei et al. 5)

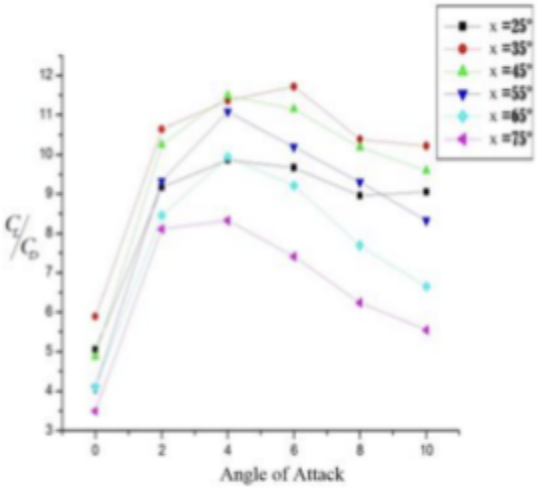

Fig 16: Lift-Drag Ratio with the AOA Ma=1.4

(Lei et al. 5)

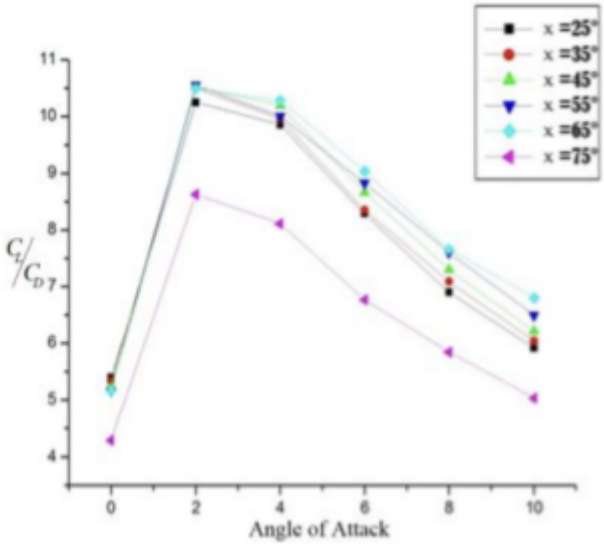

Fig 17: Lift-Drag Ratio with the AOA Ma=1.4

(Lei et al. 5)

This data suggests that there are maximum L/D ratios at different speeds and that the sweep angle of the optimum lift to drag ratio increases with speed.

3.2 Investigation

To test my hypothesis I tested the sweep angles 0°, 7.5°, 15°, 22.5°, 30°, 45° and 60°. These were chosen because the majority of civil aircraft use a range of 0-30°, however 45-60° were also considered because some high speed aircraft have much more aggressive angles that help to visualize the trend (material has same properties despite differing colors).

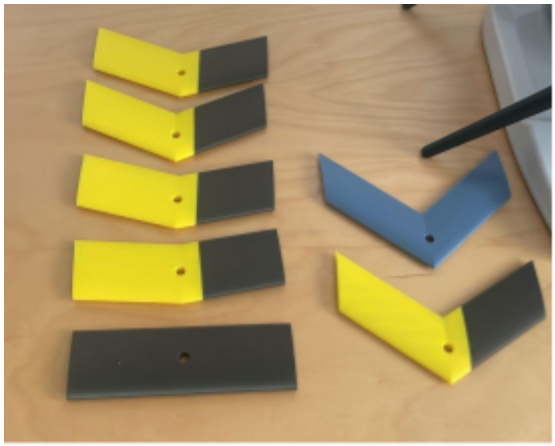

Fig 18: 7 3D Printed Wings (own image)

Additionally, because platform area is proportional to lift (Equation 1), it was controlled in this experiment during the design of the airfoils using CAD software. NACA 0015, a symmetrical foil, was used in this experiment: firstly, because it has a relatively large camber, giving a higher drag than a thinner wing and therefore a trend would be more significant; secondly a supercritical (asymmetrical) wing was avoided because they are optimized for supersonic flight which is not possible with my equipment ("Supercritical Aerofoils").

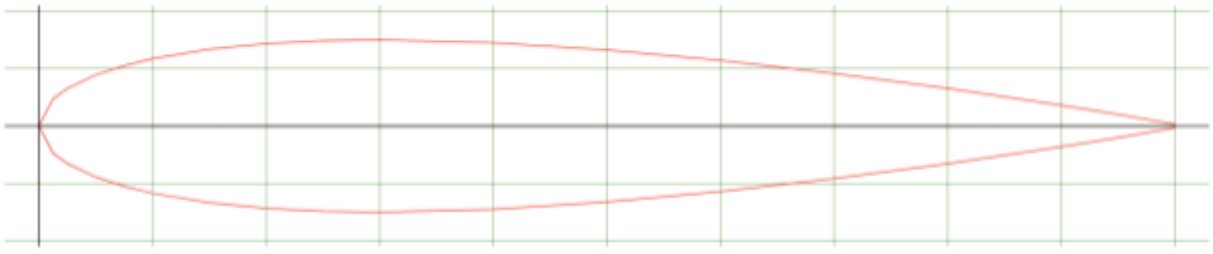

Figure 19: NACA 0015 Airfoil Diagram ("NACA 0015")

To measure lift, a preliminary experiment was conducted with a small circular piece of wood on a stand. Wings were then printed see with a circular hole in the center with an angle of attack of

five degrees; this angle of attack was chosen because this experiment is considering the environmental implications of wing sweep angles and commercial planes spend the majority of their time and fuel at cruising altitude which a source stated is approximately 5 degrees (Scott "Cruise AOA For Major Airliners"). The wing was placed inside a wind tunnel see Figure 20 with a leaf blower with variable speeds attached to the front (Figure 21).

Figure 20: First Wind Tunnel Design (own image)

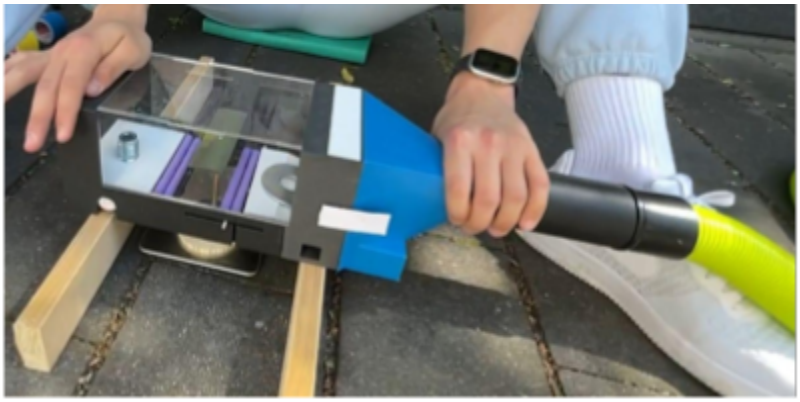

Figure 21: Preliminary Wind Tunnel (own image)

Figure 22: Laminar Flow Filter (own image)

This wind tunnel and leaf blower were initially chosen because the air outlet of the leaf blower had approximately the same size as the wingspan of the wing which would mean that the wing would feel a roughly equal airspeed across its leading edge. A small hexagonal laminar flow filter was placed in the air flow to reduce turbulence (Figure 22). In this initial experiment a max was found at 22.5 degrees (see Appendix 5). This did not agree with research because Figures 10 and 11 show that lift should decrease with sweep angle. A

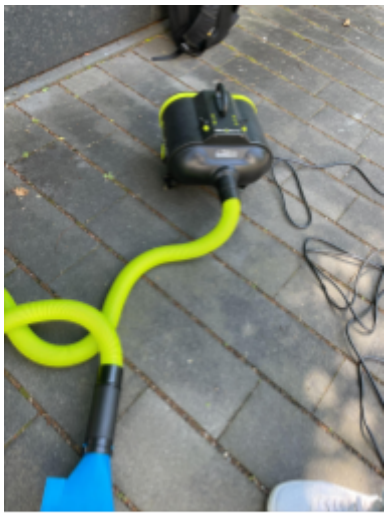

Figure 23: Prelim Leaf Blower (own image)

circular wind tunnel was designed instead to limit the material usage from multiple prints and to fit the shape of the straw filter more optimally, and to allow paper to optimally wrap around the wind tunnel easily (Figure 24 (a)).

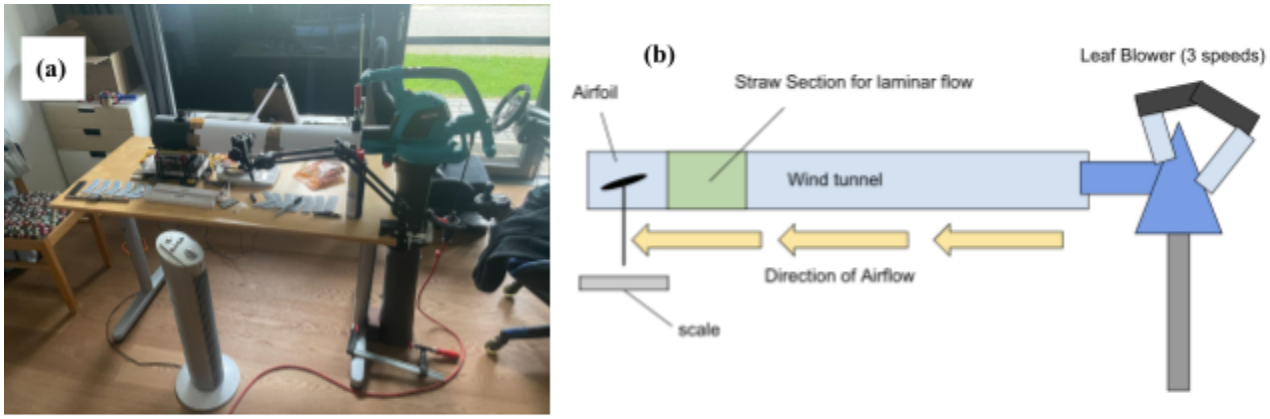

Figure 24: Final Iteration Apparatus and Diagram (own images)

To achieve more accurate results a new apparatus was constructed with a similar setup, except this time with a longer wind tunnel partially constructed of paper card and partially 3D printed (see Figure 24).

Figure 25: Wind Tunnel with Anemometer (own images)

A small opening on the top of the tunnel was designed to allow an anemometer (see Figure 25) to fit inside to measure wind speeds. The leaf blower available had 3 speeds 11,17,18.5 m/s (Measured using anemometer; 10 trials each showed consistent air speed) and was fastened to the table that the wind tunnel was placed on to minimize its movement and to control its

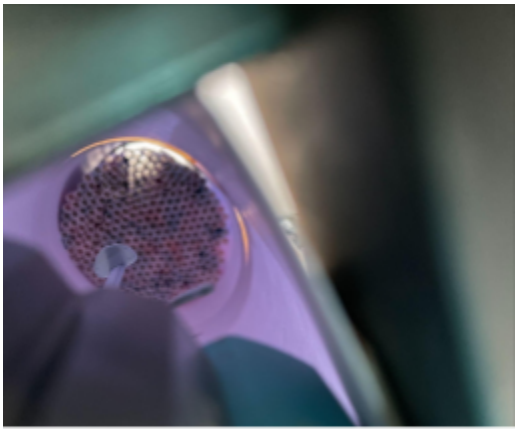

Figure 26: Laminar Flow Straw Filter (own image)

position, which was measured with a level and aimed directly into the tunnel. The leaf blower was also clamped to the end of the tunnel to limit movement of the wind tunnel and keep their relative positions controlled. Because turbulence was a problem in preliminary trials, straws were used as a laminar flow filter (see Figure 26 and 30). The connection between the stand and the wing was also redesigned with a rectangular joint to prevent the wing from rotating during data collection. Because of movement of the stand on top of the scale due to turbulence and lift, it was taped to the scale to limit movement (brown tape can be seen in Figure 25a).

Figure 27: Prelim Drag Apparatus Component (own image)

For drag data collection many different methods were tested until good results were achieved. Preliminary testing involved placing a lever arm design with rotating on a LEGO rod on top of the scale and using the torque provided by the airflow to generate a mass reading (Figure 27). This provided evidence of a small difference between different sweep angles but was too rudimentary to get accurate results.

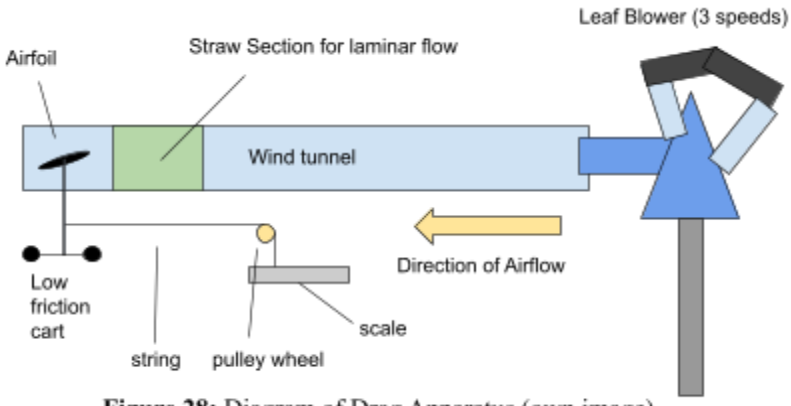

Figure 28: Diagram of Drag Apparatus (own image)

The refined experiment involved 3D printing a cart with wheels fixed on rails so that it could only move forwards and backwards to limit any rotation of the wing with a string attached to the pole of the stand (Figures 29 and 30). This string was then routed onto a wheel acting as a pulley system suspended above a scale (Figure 31). When a force was applied onto the wing from oncoming air in the form of skin and form drag, the string would be put under tension and a force was measured on the scale. For optimal results, a specific type of lego wheel was used to minimize friction and non elastic nylon string was used to limit the effects of elasticity and plastic deformation of the string (Figure 31).

Figure 29: Drag Cart (own image)

Figure 30: Exhaust-Side Tunnel View (own image)

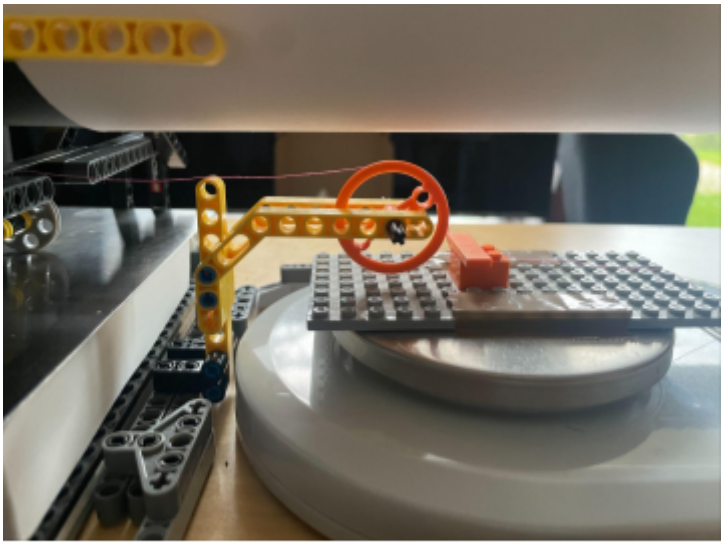

Figure 31: Drag Pulley System (own image)

3.3 Analysis & Conclusion

Table 1: Raw Data for Sweep Angle Against Lift

Windspeed ±0.1 /ms^{-1}	Sweep Angle ±0.5/°	Mass ±0.01/ g									
		T1	T2	T3	T4	T5	T6	T7	T8	T9	T10
11.0	0.0	8.75	8.76	8.82	8.81	8.72	8.61	8.93	8.73	8.84	8.75
	7.5	8.66	8.75	8.69	8.62	8.70	8.87	8.75	8.73	8.75	8.77
	15.0	8.62	8.57	8.58	8.54	8.46	8.47	8.54	8.55	8.57	8.50
	22.5	8.41	8.44	8.42	8.34	8.33	8.30	8.33	8.39	8.32	8.29
	30.0	7.90	7.93	7.91	7.90	7.93	7.97	8.10	8.08	8.00	8.12
	45.0	7.39	7.46	7.33	7.38	7.45	7.43	7.49	7.48	7.55	7.54
	60.0	6.24	6.32	6.30	6.17	6.18	6.15	6.09	6.16	6.20	6.14
17.0	0.0	21.24	21.29	21.14	20.94	20.99	21.11	21.04	21.01	21.15	21.03
	7.5	18.66	18.64	18.68	18.75	18.60	18.51	18.70	18.68	18.61	18.69
	15.0	18.53	18.64	18.72	18.74	18.60	18.39	18.31	18.22	18.30	18.46
	22.5	18.44	18.40	18.34	18.17	18.27	18.43	18.28	18.38	18.33	18.24
	30.0	17.21	17.27	17.21	17.28	17.53	17.45	17.28	17.15	17.28	17.27
	45.0	16.28	16.07	15.99	16.14	16.16	16.10	16.12	16.18	16.19	16.29
	60.0	13.24	13.26	13.28	13.21	13.32	13.43	13.41	13.30	13.15	13.18
18.5	0.0	23.83	23.67	23.50	23.67	23.88	23.87	23.71	23.63	23.77	23.60
	7.5	22.65	22.75	22.91	22.75	22.45	22.55	22.63	22.75	22.94	22.51
	15.0	22.27	22.36	22.30	22.23	22.19	22.37	22.23	22.29	22.32	22.25
	22.5	22.11	22.04	22.11	21.98	21.93	21.97	22.02	21.90	22.01	21.99
	30.0	20.53	20.69	20.73	20.47	20.48	20.42	20.48	20.62	20.72	20.69
	45.0	19.29	19.32	19.49	19.51	19.41	19.19	19.56	19.48	19.50	19.48
	60.0	16.20	16.39	16.04	15.92	16.11	15.88	15.75	15.86	16.01	16.10

Table 2: Table of Processed Data for Sweep Angle Against Lift to Drag Ratio

Sweep Angle / ±0.5°	Lift/Drag at different wind speeds					
	Wind Speed 11 ±0.1ms^{-1}		Wind Speed 17 ±0.1ms^{-1}		Wind Speed 18.5 ±0.1ms^{-1}	
	Avg.	Δ	Avg.	Δ	Avg.	Δ
0.0	9	1	10	1	10	1
7.5	9	1	9	1	10	1
15.0	9	1	9	1	9	1
22.5	10	1	9	1	9	1
30.0	13	1	11	1	9	1
45.0	15	2	9	1	9	1
60.0	11	1	10	1	10	1

Table 1 is the final raw data from my lift collection attempts and table 2 shows the final processed data for Lift/Drag ratio as graphed in Figure 34. All other raw and processed data can be found in Appendices 1-5.

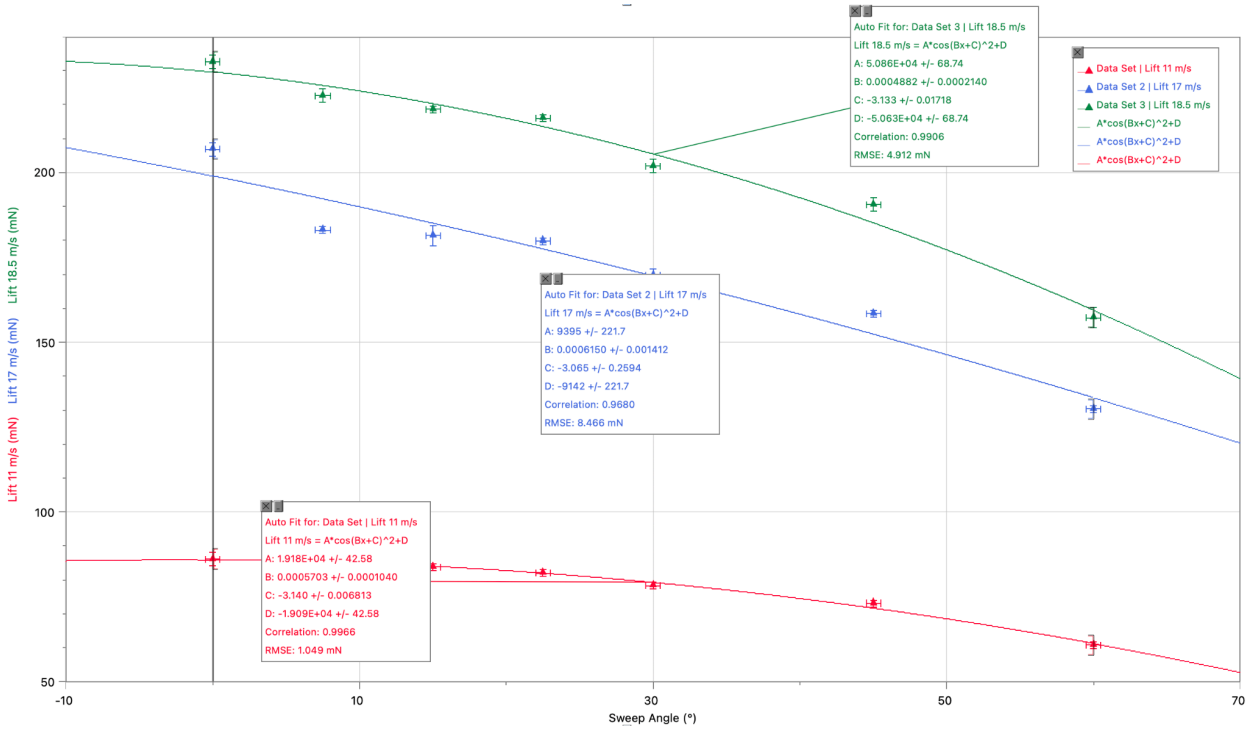

Fig 32: Graph of Sweep Angle Against Lift for Different Subsonic Wind Speeds

This investigation aimed to determine the optimum L/D ratio for a plane at subsonic air speeds. The first component in determining this is determining the lift of the wing. Based on literature and airflow behavior, it was predicted in the hypothesis (page 11) that the lift would consistently decrease with increasing sweep angles after 0°. Figure 32 demonstrates this for all three windspeeds. Figure 32 also illustrates that the rate of decrease in lift, when fit with a cos^2 relationship, increases as speed increases. This suggests that, if a plane is intended to fly at higher speeds, sweep angle will play an increasingly important role in determining the amount of lift experienced by the aircraft.

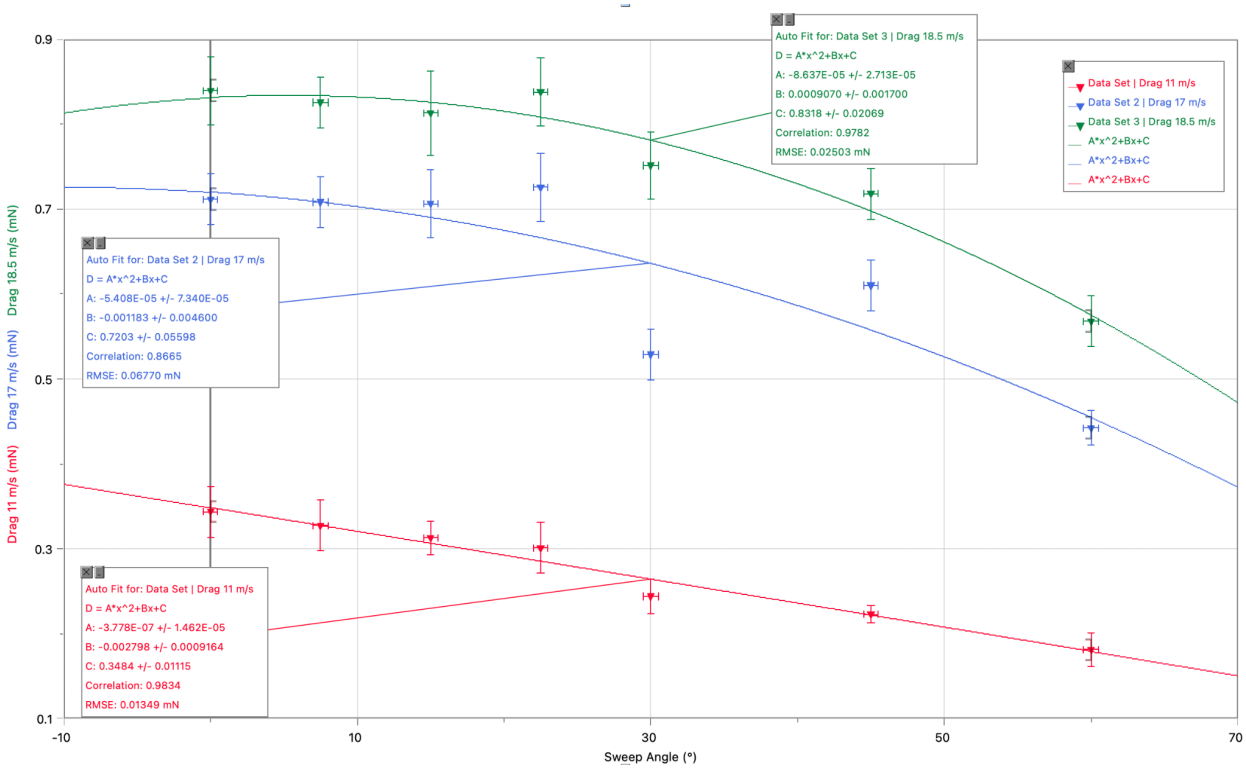

Fig 33: Graph of Sweep Angle Against Drag for Different Subsonic Wind Speeds

The second component in determining the optimum L/D ratio is the drag. For drag it was predicted (page 13) that it would also consistently decrease with increasing sweep angles after 0° which has clearly been shown to be true. It can also be seen that drag has a nearly perfect linear relationship at low speeds, whereas at high speeds drag has a steep decrease after approximately 30° sweep angle. In a real world context, this indicates that planes with a super high speed envelope would experience far greater drag benefits with sweep angles greater than 30°, allowing for increasingly optimized fuel consumption.

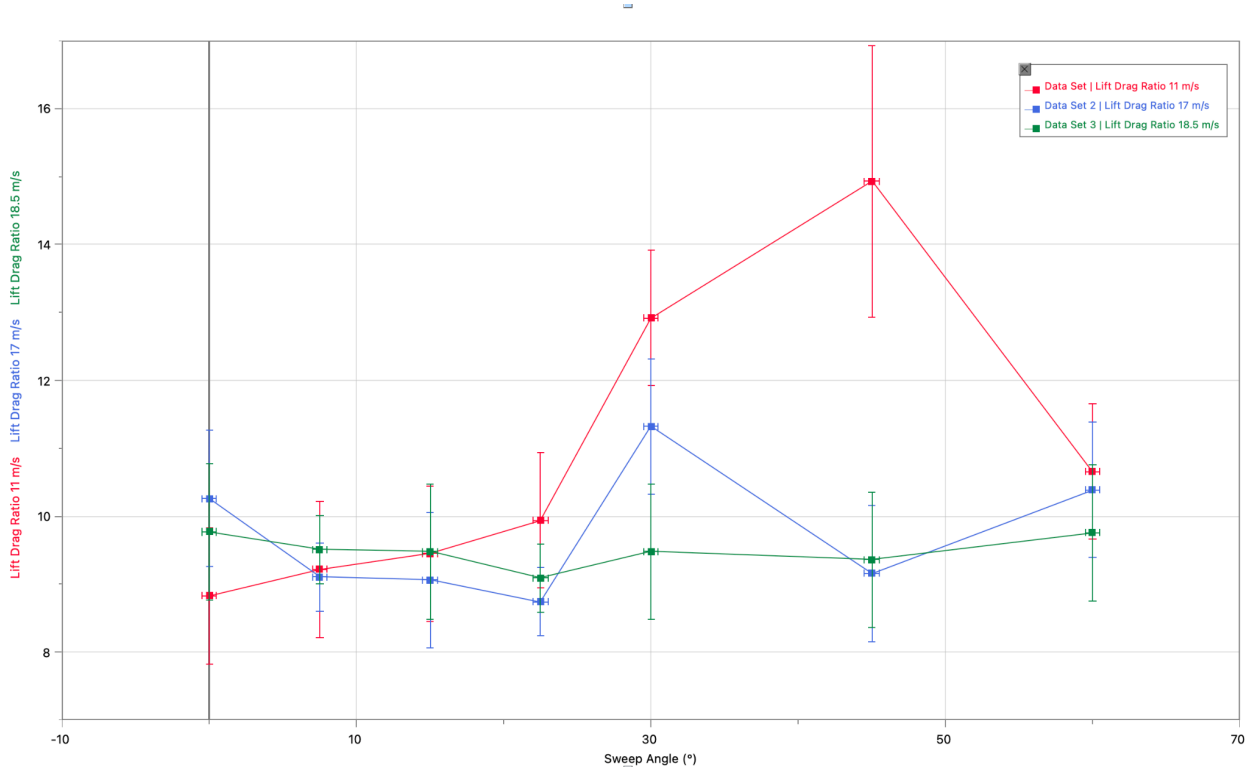

Fig 34: Graph of Sweep Angle Against Lift to Drag Ratio for Different Subsonic Wind Speeds

The lift/drag ratio data did not show any conclusive trend throughout all speeds, however it showed a maximum sweep angle at 45° for low speeds, a smaller maximum at 30° for medium speed and no clear maximum for high speeds. This conflicts with the hypothesis which predicted

that the opposite would happen; it predicted that the sweep angle of the optimum lift to drag ratio increases with speed. Due to the relatively low error, it can be said that these results are valid and that the trends observed in literature just were not applicable to this low airspeed region. One source (Chen) did find that “at Mach 0.4 and 0.6, the relationship between sweep angle and lift-drag ratio is not significant and fluctuates up and down”. As these were the lowest speeds tested, it could be extrapolated that this would apply to much lower speeds such as those used in this experiment, but the lack of unreasonably high uncertainty in this experiment suggests these results should still be considered valid. Additionally, the data can be considered valid due to the lift/drag ratios falling within expected values for real airfoils (Filippone).

3.4 Evaluation

Due to the number of variables and lack of specialized equipment, there are numerous ways to improve this experiment.

Firstly, due to the difference in width of the nozzle of my leaf blower, the distribution of pressure within the tunnel could not be perfectly balanced. To combat this, a longer wind tunnel was constructed to allow the air to disperse more evenly throughout; however, due to the high speeds of the leaf blower, this effect, which is very difficult to quantify (it can only be seen as reduced turbulence/less fluctuations on the scale), is still prevalent leading to minor turbulence and uneven airflow over the airfoil. This could be improved by using a larger air flow source for the wind tunnel, such as a large fan with a size similar to the diameter of the tunnel.

The tool used for airflow generation was a leaf vacuum, with the container for leaves removed to function as a leaf blower. However, because it was originally a vacuum and the long nozzle is not detachable, its intake nozzle was placed on the ground with small gaps available for intake, leading to a less efficient output and lower air speeds over the airfoil (see Figure 24). The leaf blower could have been elevated to increase its efficiency, but the increase in efficiency was found to be negligible during testing and would have come at the cost of increased vibrations and instability of the entire apparatus; therefore, the leaf blower was placed in contact with the ground. The nozzle was also designed with small gaps so there would not be a complete air seal which allowed the leaf blower to get sufficient air for the experiment. The effect of the leaf blower being on the ground can be considered to have very minimal to no effect on the experiment.

Despite efforts to control as much as possible, numerous uncertainties were inevitable in terms of the wings themselves. Controlling the AoA of attack depended on the table being level, the surface upon which the stand was placed, the AoA of each wing as they were printed and the angle of the oncoming air from the leaf blower which effectively changes the angle of attack as well. To control surfaces being level, a mechanical level was used, as well as the digital level built into an iphone when initially setting up the apparatus. Due to the wings being 3D printed and designed on Fusion 360 (a CAD modeling software) the AoA of attack of the wing relative to the bottom of the stand which was also 3D printed can be considered accurate, as the Bambu X1 carbon can print with 0.2 mm accuracy. Lastly the level of the leaf blower was controlled by clamping it to the table and also controlling that the nozzle pointing into the wind tunnel was

found to be level using the aforementioned method. If this experiment were conducted with better equipment and a larger, more powerful air flow source, (The wings printed were small in this experiment because the strongest available air source had a very small nozzle--the wings were kept to 10cm width to keep their width close to the width of the nozzle so the air would be evenly distributed across the airfoil for optimal results) the small fluctuations of the AoA could be reduced by using larger wings for testing. This would significantly reduce the relative turbulence effects and decrease any uncertainties in relation to the lift/drag measurements.

The sweep angle of each wing was well controlled as the wings were 3D printed to high precision and accuracy; however, the wing and the stand would often rotate, changing the effective sweep angle of each wing against the oncoming airflow. This was controlled by taping the stand to the scale which was fixed by 4 lego pieces on each corner. Due to the adjustable design of the wings and the stand for this experiment, where each wing could be taken off and swapped to save materials, there were small gaps on the point where the wings would be attached to the stand. This means that there was still a small amount of potential side to side vibration of the wing, adding to the uncertainty. This could have also been controlled more effectively if bigger wings were used as the fluctuations, as mentioned before, would in relation to the measurements, have minor effects.

The scale in this experiment had a high degree of accuracy (±0.01g) which, relative to the turbulence conditions, was sufficiently accurate to the point where an increase in measuring capability would likely not have increased the validity of the data.

The laminar flow filter used was a collection of straws of 15 cm length. Perhaps a more sturdy 3D printed form would have reduced any turbulence in the airflow. This is of course contingent on the source of the air flow creating a dispersed enough flow that all of the straws experience equal pressure and air flow conditions.

Uncertainties within the string were a given as any available type had some amount of elasticity. To control this effect, the length of the string used in the pulley system was kept to a minimum to reduce the total amount of stretch within the string. The string may have also had some stretching occur past the point of plastic deformation which would alter the readings on the scale as the cart would be able to move further back and the wind would be slightly lower the further the cart gets from the leaf blower/source of the air. Nonetheless, a material such as kevlar or steel wire could be substituted and may result in reduced uncertainty. Additionally, because the drag measurements had such small values (0.1-0.2g) even this small of an improvement in control could make a noticeable difference.

It's also likely that the lego wheels used had some surface imperfections that may have caused small inaccuracies, especially at such low weight. Overall, especially for the drag measurements, digital measuring and simulation tools such as Computational Fluid Dynamics (CFD) would be a good alternative to get theoretical results, eliminating any experimental uncertainty in the apparatus.

Section 4: Discussion

In conclusion, it would be most advantageous to have minimally swept back wings during takeoff to maximize lift while gaining altitude, then at high altitude it would be most optimal to have high angle swept back wings. This conclusion is corroborated by the design of the Grumman F-14 Tomcat (see Figures 35 and 36) because this plane has variable sweep back angles for different situations.

Figure 35: F-14 with Swept Back Wings (Scott "F-14 Wing Sweep & Aspect Ratio")

Figure 36: F-14 with Unswept Wings (Taylor)

Works Cited

"Ask an Explainer." *How Things FLy*, National Air and Space Museum, 31 Mar. 2017, howthingsfly.si.edu/ask-an-explainer/how-are-swept-back-wings-vs-straight-wings-effected-aerodynamics-and-one-model-supe. Accessed 14 Sept. 2024.

Babinsky, Holger. "How Do Wings Work?" *Physics Education*, vol. 38, no. 6, 1 Nov. 2003, pp. 497-503. *ResearchGate*, https://doi.org/10.1088/0031-9120/38/6/001. Accessed 25 Oct. 2024.

Benson, Tom. "Bernoulli and Newton." *Glenn Research Center*, NASA Glenn Research Center, www.grc.nasa.gov/www/k-12/VirtualAero/BottleRocket/airplane/bernnew.html. Accessed 25 Oct. 2024.

---. "Incorrect Theory #1." *Glenn Research Center*, NASA Glenn Research Center, www.grc.nasa.gov/www/k-12/VirtualAero/BottleRocket/airplane/wrong1.html. Accessed 25 Oct. 2024.

---. "Incorrect Theory #2." *Glenn Research Center*, NASA Glenn Research Center, www.grc.nasa.gov/www/k-12/VirtualAero/BottleRocket/airplane/wrong2.html. Accessed 25 Oct. 2024.

---. "The Lift Equation." *Glenn Research Center*, NASA Glenn Research Center, www.grc.nasa.gov/www/k-12/VirtualAero/BottleRocket/airplane/lifteq.html. Accessed 24 Oct. 2024.

Burnside, Joseph. "Theories Of Lift." *Aviation Safety*, Firecrown, 19 Mar. 2020, www.aviationsafetymagazine.com/airmanship/theories-of-lift/. Accessed 25 Oct. 2024.

Chen, Kainan. "The Performance and Application of Sweep Wing Aircraft." *Theoretical and Natural Science*, vol. 9, no. 1, 13 Nov. 2023, pp. 73-80. *researchgate*, https://doi.org/10.54254/2753-8818/9/20240719.

Cssonawala. "Lift Theories." *iamchaitanya*, 2 april 2016, iamchaitanya.wordpress.com/2016/04/02/lift-theories/. Accessed 25 Oct. 2024.

Filippone, A., editor. "Lift-to-Drag Ratios." *Aerodyn.org*, A. Filippone, 2005, aerodyn.org/ld-tables/. Accessed 27 Oct. 2024.

"Friction Drag." *SkyBrary*, SKYbrary Aviation Safety., 2021, skybrary.aero/articles/friction-drag. Accessed 25 Oct. 2024.

Hall, Nancy, editor. "Modern Drag Equation." *Glenn Research Center*, edited by Marcelo Dasilva, NASA, Jan. 2023, www1.grc.nasa.gov/beginners-guide-to-aeronautics/modern-drag-equation/#:~:text=The%20drag%20equation%20states%20that,the%20wing%20area%20(A). Accessed 28 Sept. 2024.

---, editor. "What is Drag?" *Glenn Research Center*, edited by Marcelo Dasilva, NASA Glenn Research Center, 21 July 2022, www1.grc.nasa.gov/beginners-guide-to-aeronautics/what-is-drag/#:~:text=We%20can%20think%20of%20drag,of%20both%20solid%20and%20gas. Accessed 25 Oct. 2024.

---, editor. "What is Lift?" *Glenn Research Center*, edited by Marcelo Dasilva, NASA Glenn Research Center, 21 July 2022, www1.grc.nasa.gov/beginners-guide-to-aeronautics/what-is-lift/#:~:text=Lift%20is%20a%20mechanical%20force,without%20being%20in%20physical%20contact. Accessed 25 Oct. 2024.

HappyApple. "Venturi Effect." *Wikipedia*, Wikimedia Foundation, 22 Sept. 2024, en.wikipedia.org/wiki/Venturi_effect#/media/File:Venturi5.svg. Accessed 25 Oct. 2024.

Jing, Zhenrong, and Zhangfeng Huang. "Instability Analysis and Drag Coefficient Prediction on a Swept RAE2822 Wing with Constant Lift Coefficient." *Chinese Journal of Aeronautics*, vol. 30, no. 3, June 2017, pp. 964-75. *ScienceDirect*, https://doi.org/10.1016/j.cja.2017.03.002.

Lei, Yuchang, et al. "Numerical Study on Aerodynamic Characteristics of Variable-sweep Morphing Aircraft at Transonic Speeds." *IOP Conference Series: Materials Science and Engineering*, vol. 751, no. 1, 1 Jan. 2020, p. 012001. *IOPScience*, https://doi.org/10.1088/1757-899x/751/1/012001.

"NACA 0015 (naca0015-il)." *Airfoil Tools*, airfoiltools.com/airfoil/details?airfoil=naca0015-il. Accessed 25 Oct. 2024.

Scott. "Cruise AOA For Major Airliners." *Airliners.net*, 2006, www.airliners.net/forum/viewtopic.php?t=749969. Accessed 24 Oct. 2024.

Scott, Jeff. "F-14 Wing Sweep & Aspect Ratio." *Aerospaceweb.org*, 30 july 2006, aerospaceweb.org/question/aerodynamics/q0281c.shtml. Accessed 24 Oct. 2024.

Smits, Alexander J. "Bernoulli's Equation." *Aerodynamics of Bicycles*, Princeton University, swh.princeton.edu/~asmits/Bicycle_web/Bernoulli.html. Accessed 25 Oct. 2024.

"Supercritical Aerofoils." *SkyBrary*, SKYbrary Aviation Safety, skybrary.aero/articles/supercritical-aerofoils. Accessed 24 Oct. 2024.

"Swept Wings | Simple Explanation of a Complex Topic." *YouTube*, uploaded by Flight-Club, 18 July 2023, www.youtube.com/watch?v=11nz0YZSNxw&t=3s. Accessed 25 Sept. 2024.

Taylor, Rob. *An F-14D Tomcat conducts a mission over the Persian Gulf region*. 5 Nov. 2005. *Wikipedia*, en.wikipedia.org/wiki/Grumman_F-14_Tomcat. Accessed 24 Oct. 2024.

Wood, Andrew. "Sweep Angle and Supersonic Flight." *AeroToolbox*, Canard Analytics, 28 Sept. 2022, aerotoolbox.com/intro-sweep-angle/. Accessed 11 Sept. 2024.

Zeng, Lifang, et al. "Mechanism Analysis of Hysteretic Aerodynamic Characteristics on Variable-sweep Wings." *Chinese Journal of Aeronautics*, vol. 36, no. 5, May 2023, pp. 212-22. *ScienceDirect*, https://doi.org/10.1016/j.cja.2023.01.002. Accessed 27 Oct. 2024.

Appendix 1: Table of Processed Data for Sweep Angle against Lift

Sweep Angle / ±0.5°	Lift at different wind speeds					
	Wind Speed 11 ±0.1ms^{-1}		Wind Speed 17 ±0.1ms^{-1}		Wind Speed 18.5 ±0.1ms^{-1}	
	Avg.	Δ	Avg.	Δ	Avg.	Δ
0.0	86.1	2	206.9	2	232.6	2
7.5	85.6	1	183.0	1	222.6	2
15.0	83.8	1	181.4	3	218.6	1
22.5	82.0	1	179.8	1	215.9	1
30.0	78.3	1	169.6	2	201.9	2
45.0	73.1	1	158.5	1	190.5	2
60.0	60.8	1	130.3	1	157.2	3

Appendix 2: Table of Processed Data for Sweep Angle against Drag

Sweep Angle / ±0.5°	Drag at different wind speeds					
	Wind Speed 11 ±0.1ms^{-1}		Wind Speed 17 ±0.1ms^{-1}		Wind Speed 18.5 ±0.1ms^{-1}	
	Avg.	Δ	Avg.	Δ	Avg.	Δ
0.0	9.74	1	20.17	1	23.81	1
7.5	9.28	1	20.08	1	23.41	1
15.0	8.87	1	20.02	1	23.06	1
22.5	8.25	1	20.58	1	23.75	1
30.0	6.06	1	14.99	1	21.30	1
45.0	4.89	1	17.30	1	20.36	1
60.0	5.70	1	12.54	1	16.10	1

Appendix 3: Table of Raw Data Prelim Testing for Lift

Prelim Testing/Tuning at Home Apparatus				Subvalues for Trials (-g)									
Sweep Angle +/- 0.5°	**Leaf Blower**	**Wind Speed (m/s) +/- 0.1**	**Lift Average (-g) ±0.01g**	**1**	**2**	**3**	**4**	**5**	**6**	**7**	**8**	**9**	**10**
7.5	MIN	11.0	17.43	17.27	17.24	17.34	17.42	17.49	17.37	17.46	17.53	17.64	17.58
7.5	MIN	11.0	17.23	17.37	17.25	17.08	17.07	17.10	17.28	17.17	17.12	17.41	17.49
7.5	MIN	11.0	17.53	17.17	17.35	17.51	17.71	17.68	17.63	17.54	17.5	17.58	17.65
15	MIN	11.0	18.89	18.91	18.95	19.16	19.24	18.96	18.81	18.72	18.64	18.68	18.80
15	MIN	11.0	18.54	18.58	18.54	18.31	18.5	18.56	18.59	18.53	18.51	18.64	18.60
15	MIN	11.0	18.49	18.51	18.58	18.59	18.46	18.42	18.46	18.58	18.60	18.37	18.31
22.5	MIN	11.0	18.81	18.63	18.76	18.74	18.88	18.99	18.88	18.70	18.85	18.86	18.81
22.5	MIN	11.0	18.53	18.42	18.34	18.52	18.54	18.61	18.63	18.72	18.64	18.38	18.47
22.5	MIN	11.0	18.65	18.31	18.49	18.64	18.58	18.74	18.86	18.78	18.84	18.85	18.44
30	MIN	11.0	17.38	17.28	17.19	17.16	17.34	17.49	17.54	17.43	17.29	17.46	17.63
30	MIN	11.0	17.28	17.59	17.42	17.27	17.12	17.11	17.17	17.31	17.36	17.23	17.17
30	MIN	11.0	17.30	17.54	17.23	17.16	17.20	17.30	17.25	17.28	17.40	17.32	17.27
45	MIN	11.0	17.03	16.95	16.82	17.05	17.14	16.97	16.92	17.00	17.22	17.19	17.05
45	MIN	11.0	17.00	17.05	17.00	16.91	17.24	16.96	16.98	16.95	16.99	16.97	16.91
45	MIN	11.0	17.10	17.23	17.22	17.09	17.03	17.07	16.94	16.98	17.17	17.19	17.04
60	MIN	11.0	14.83	14.67	14.72	14.84	14.82	14.86	14.82	14.86	14.91	14.93	14.87
60	MIN	11.0	14.82	14.68	14.71	14.69	14.70	14.86	14.91	14.84	14.91	14.99	14.93
60	MIN	11.0	14.97	15.02	15.12	15.05	15.06	15.00	14.97	14.87	14.84	14.83	14.97

Appendix 4: Table of Raw Data for Drag

Prelim Testing/Tuning at Home Apparatus			**Subvalues for Trials (-g)**										
Sweep Angle +/- 0.5°	**Wind Speed (m/s) +/- 0.1**	**Drag Average (-g) ±0.01g**	**1**	**2**	**3**	**4**	**5**	**6**	**7**	**8**	**9**	**10**	Δ
0	11.0	3.49	3.52	3.45	3.56	3.47	3.51	3.57	3.39	3.43	3.54	3.44	3.49
7.5	11.0	3.44	3.49	3.42	3.45	3.47	3.40	3.50	3.44	3.43	3.46	3.37	3.44
15	11.0	3.40	3.37	3.40	3.37	3.44	3.36	3.43	3.40	3.41	3.38	3.42	3.40
22.5	11.0	3.34	3.18	3.29	3.32	3.35	3.43	3.40	0.00	3.35	3.37	3.35	3.34
30	11.0	3.11	3.06	3.12	3.18	3.20	3.09	3.15	3.06	3.09	3.12	3.06	3.11
45	11.0	2.99	2.92	2.95	2.98	3.03	3.01	3.06	3.03	2.95	2.98	3.03	2.99
60	11.0	3.08	2.95	2.98	3.01	3.06	3.12	3.18	3.20	3.09	3.12	3.06	3.08
0	17.0	7.23	7.26	7.20	7.29	7.19	7.25	7.32	7.14	7.16	7.27	7.18	7.23
7.5	17.0	7.22	7.12	7.23	7.17	7.20	7.26	7.29	7.20	7.12	7.29	7.31	7.22
15	17.0	7.21	7.29	7.14	7.34	7.29	7.26	7.12	7.14	7.20	7.06	7.29	7.21
22.5	17.0	7.27	7.23	7.20	7.37	7.31	7.29	7.31	7.17	7.12	7.40	7.29	7.27
30	17.0	6.70	6.75	6.83	6.66	6.55	6.72	6.83	6.72	6.61	6.69	6.63	6.70
45	17.0	6.93	6.83	6.80	6.95	6.97	6.83	6.92	7.00	7.06	7.14	6.83	6.93
60	17.0	6.45	6.35	6.38	6.41	6.44	6.32	6.49	6.46	6.58	6.55	6.52	6.45
0	18.5	8.69	8.82	8.76	8.53	8.62	8.65	8.73	8.53	8.59	8.82	8.85	8.69
7.5	18.5	8.65	8.69	8.59	8.73	8.63	8.67	8.74	8.56	8.58	8.68	8.61	8.65
15	18.5	8.61	8.33	8.62	8.73	8.67	8.56	8.53	8.48	8.67	8.85	8.67	8.61
22.5	18.5	8.68	8.70	8.73	8.79	8.82	8.76	8.56	8.45	8.59	8.73	8.70	8.68
30	18.5	8.43	8.25	8.31	8.33	8.48	8.50	8.53	8.62	8.45	8.42	8.45	8.43
45	18.5	8.34	8.36	8.25	8.39	8.48	8.45	8.36	8.25	8.31	8.19	8.33	8.34
60	18.5	7.90	7.91	7.77	7.99	8.08	7.91	7.85	7.74	7.88	7.91	7.99	7.90
Apparatus low	11.0	2.49	2.32	2.35	2.41	2.47	2.49	2.52	2.61	2.64	2.58	2.55	2.49
Apparatus med	17.0	5.17	5.22	5.19	5.07	5.16	5.10	5.05	5.07	5.19	5.30	5.36	5.17
Apparatus high	18.5	6.26	6.10	6.24	6.15	6.10	6.27	6.32	6.35	6.38	6.44	6.29	6.26

Appendix 5: Table of Preliminary Data with First Apparatus Iteration

Sweep Angle +/- 0.5°	Leaf Blower Power Setting				
	Low	High	Low-Low	Low-High	High-High
	Lift (-g) +/- 1				
0°	4	4	33	40	38
0°	4	3	31	34	35
0°	3	3	32	33	35
Average	3.7	3.3	32.0	35.7	36.0
7.5°	5	4	34	32	33
7.5°	5	4	31	32	35
7.5°	4	4	34	29	32
Average	4.7	4.0	33.0	31.0	33.3
15°	7	8	35	37	30
15°	6	8	37	38	36
15°	5	6	36	33	33
Average	6.0	7.3	36.0	36.0	33.0
22.5°	5	8	42	32	40
22.5°	5	6	37	39	41
22.5°	7	9	36	40	42
Average	5.7	7.7	38.3	37.0	41.0
30°	6	7	37	35	37
30°	5	7	35	38	38
30°	5	5	36	33	35
Average	5.3	6.3	36.0	35.3	36.7
45°	5	6	33	33	37
45°	4	6	31	31	36
45°	5	4	33	29	34
Average	4.7	5.3	32.3	31.0	35.7
60°	4	5	38	34	39
60°	5	5	36	39	40
60°	4	5	37	37	39
Average	4.3	5.0	37.0	36.7	39.3